

Joint Reward Modeling: Internalizing Chain-of-Thought for Efficient Visual Reward Models

Yankai Yang^{1*} Yancheng Long^{1*} Hongyang Wei² Wei Chen³ Tianke Zhang⁴ Kaiyu Jiang⁴ Haonan Fan⁴ Changyi Liu⁴ Jiankang Chen⁴ Kaiyu Tang⁴ Bin Wen^{4†} [✉] Fan Yang⁴ Tingting Gao⁴ Han Li⁴ Shuo Yang^{1✉}

Website: <https://github.com/Kwai-Keye/JRM-Joint-Reward-Modeling>

Abstract

Reward models are critical for reinforcement learning from human feedback, as they determine the alignment quality and reliability of generative models. For complex tasks such as image editing, reward models are required to capture global semantic consistency and implicit logical constraints beyond local similarity. Existing reward modeling approaches have clear limitations. Discriminative reward models align well with human preferences but struggle with complex semantics due to limited reasoning supervision. Generative reward models offer stronger semantic understanding and reasoning, but they are costly at inference time and difficult to align directly with human preferences. To this end, we propose **Joint Reward Modeling (JRM)**, which jointly optimizes preference learning and language modeling on a shared vision-language backbone. This approach internalizes the semantic and reasoning capabilities of generative models into efficient discriminative representations, enabling fast and accurate evaluation. JRM achieves state-of-the-art results on MMRB2 and EditReward-Bench, and significantly improves stability and performance in downstream online reinforcement learning. These results show that joint training effectively bridges efficiency and semantic understanding in reward modeling.

1. Introduction

Reward models are a core component of reinforcement learning from human feedback (RLHF) frameworks (Liu et al.,

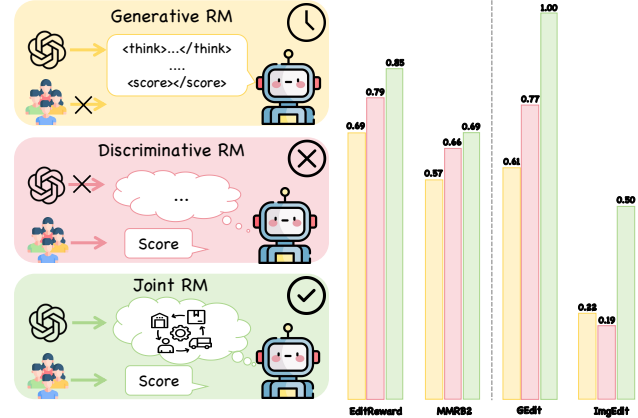


Figure 1. Performance comparison. **Left:** Comparison of Generative, Discriminative, and Joint Reward Modeling (JRM) paradigms. **Right:** JRM achieves state-of-the-art accuracy on benchmarks and significantly boosts downstream RL performance. Note: in the performance comparison, Generative RM refers to EditScore (Luo et al., 2025), and Discriminative RM refers to EditReward (Wu et al., 2025d).

2025a; Xue et al., 2025). Their primary role is to map human preferences into optimizable scalar signals, which support stable policy alignment. As multimodal foundation models evolve from perception toward reasoning and content creation, reward models are increasingly expected to handle complex generative tasks such as image editing. In these settings, reward models must go beyond surface-level similarity and capture global semantic consistency across regions and images, as well as implicit logical constraints.

In practice, existing reward modeling approaches mainly fall into two categories: discriminative and generative. Discriminative reward models (Wu et al., 2025d; Ma et al., 2025; Zhang et al., 2025b; 2023) typically adopt preference learning paradigms. They directly align with human preference signals using ranking loss, which gives them stable, accurate, and efficient performance in sample ranking and quality discrimination. These models naturally leverage human preference data and provide low-latency, low-variance reward feedback in reinforcement learning loops. However, their limitations are also evident. Due to the lack of rea-

^{*}Equal contribution . Work done during internship at Kuaishou.

[†] Project leader. [✉] Corresponding authors. ¹Harbin Institute of Technology, Shenzhen ²Tsinghua Shenzhen International Graduate School, Tsinghua University ³The Hong Kong University of Science and Technology ⁴Kuaishou Technology. Correspondence to: Shuo Yang <shuoyang@hit.edu.cn>, Bin Wen <wenbin@kuaishou.com>.

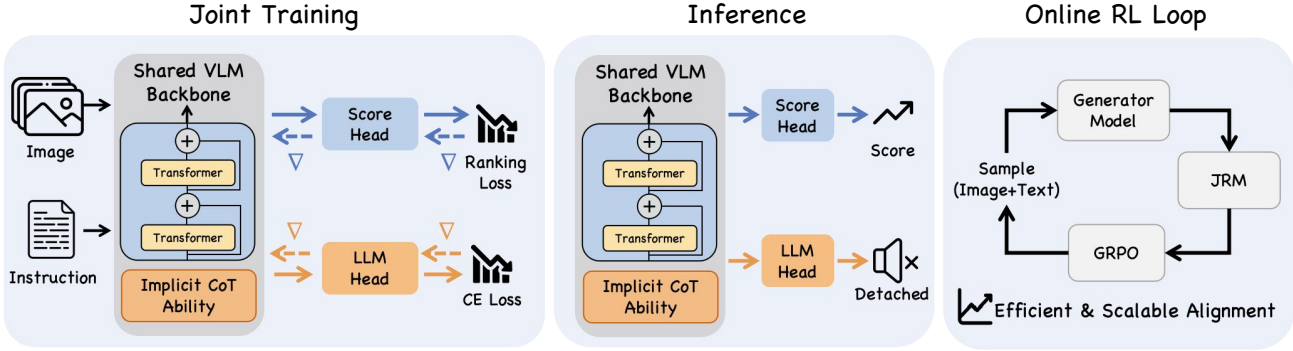


Figure 2. Illustration of the JRM Framework. The workflow consists of three stages: (1) Joint Training, where the model internalizes reasoning capabilities; (2) Efficient Inference, which retains only the discriminative pathway; and (3) the Online RL Loop, where JRM provides scalable feedback for downstream alignment.

soning supervision, discriminative reward models often rely on local visual patterns or shallow statistical cues. As a result, they struggle to capture complex semantic and logical structures, such as cross-region consistency, numerical relations, and fine-grained text-image alignment. This limits both their evaluation depth and generalization ability.

In contrast, generative reward models (Luo et al., 2025; Wu et al., 2025c; Zhang et al.; Gong et al., 2025) exhibit stronger potential in semantic understanding and reasoning. Their fundamental challenge, however, lies in preference modeling. Generative reward models are typically trained with language modeling objectives and optimized using cross-entropy loss. Their learning signals emphasize the coherence of generated reasoning text, rather than direct and fine-grained relative preference modeling among candidate samples. In real-world settings, human feedback is often provided in the form of preference comparisons or coarse selections. Such feedback rarely includes the detailed scores or accompanying reasoning texts required by generative models. This mismatch makes it difficult for generative reward models to align reliably and directly with true human preferences. Moreover, during reinforcement learning, generative reward models must repeatedly generate intermediate reasoning text, which introduces substantial computational cost and inference latency. Their reward signals are expensive and often less stable than those produced by ranking-based discriminative models, especially in sample comparison tasks. These factors together limit the practical deployment of generative reward models in large-scale online RL scenarios.

This analysis reveals a fundamental gap in current reward modeling paradigms. Generative reward models possess strong semantic understanding and reasoning capabilities, yet they struggle to effectively model and exploit human preferences. Discriminative reward models, on the other hand, align with human preferences accurately and efficiently, but lack expressive semantic and logical representa-

tions and cannot easily distill complex reasoning abilities from stronger models. This leads to a central question addressed in this work: **Is it possible to endow discriminative reward models with strong semantic understanding and reasoning ability, without sacrificing preference modeling accuracy or inference efficiency?**

Human experts typically undergo extensive explicit reasoning training before internalizing complex logic into fast and stable intuitive judgments. We argue that the reasoning ability of a reward model does not depend on whether reasoning steps are explicitly generated in language at inference time. Instead, it depends on whether relevant semantic and logical structures are effectively constructed and organized within its internal representation space. By aligning reasoning representations with discriminative features in latent space, reasoning capability can be transformed into discriminability, enabling efficient and logically consistent reward evaluation.

Based on this insight, we propose **Joint Reward Modeling (JRM)**. JRM is not a simple compromise between discriminative and generative approaches. Instead, it introduces a new reward modeling paradigm (see Figure 2). On a shared vision-language backbone, JRM jointly optimizes a ranking loss for preference learning and a cross-entropy loss for language modeling. During training, the model absorbs and internalizes semantic understanding and reasoning ability from strong models through language supervision (as visualized in Figure 3). During inference, the language generation pathway is fully removed, and only an efficient discriminative scoring mechanism is retained. This training-inference decoupling enables fast, stable, and logically grounded reward evaluation. For the first time, discriminative reward models can systematically acquire the deep semantic and reasoning capabilities of generative models.

Extensive evaluations demonstrate that JRM significantly outperforms existing state-of-the-art closed-source models with zero test-time reasoning overhead. On EditReward-

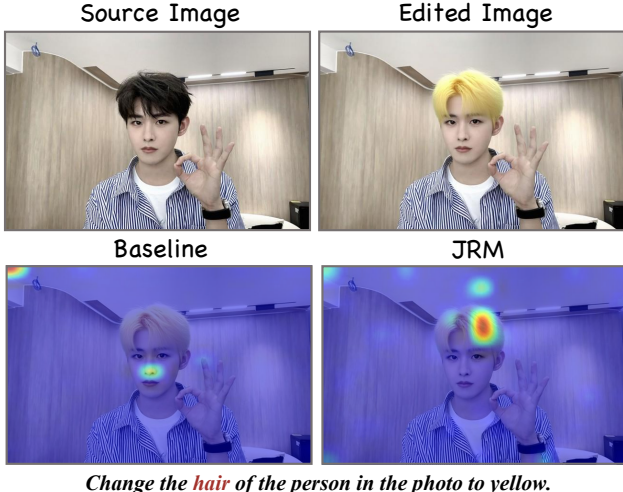


Figure 3. Attention visualization. Compared to the baseline, JRM accurately focuses on salient regions specified by editing instructions, where the baseline refers to a discriminative reward model without semantic supervision.

Bench (Wu et al., 2025d), JRM achieves an accuracy of 85.1%, **outperforming GPT-5 (75.5%) by 9.6%**. On the MMRB2 (Hu et al., 2025) benchmark, JRM reaches a composite score of 69.3%, **exceeding GPT-5 (61.9%) by 7.4%**. Further analysis shows that JRM attains an effective feature space rank of 91.77, nearly double that of the baseline (46.86), indicating that joint training alleviates representation collapse and successfully internalizes complex reasoning structures. In downstream online reinforcement learning tasks (Flow-GRPO), JRM-guided models achieve significant performance gains of **1.00** and **0.50** on GEdit-Bench and ImageEdit-Bench (Liu et al., 2025b; Ye et al., 2025), respectively, substantially outperforming the gains yielded by GPT-4.1 (+0.45 and +0.26), confirming its efficiency and robustness in real-world systems.

Our main contributions are summarized as follows:

- **We propose Joint Reward Modeling (JRM), a new paradigm that systematically equips discriminative reward models with strong semantic understanding and reasoning ability.** JRM preserves the strengths of discriminative models in preference modeling, accuracy, and inference efficiency, while inheriting the capability of generative models to handle complex semantics and logic.
- **We introduce a joint training mechanism that aligns reasoning and discriminative features in latent space.** Through shared representations and multi-objective optimization, JRM significantly enhances sensitivity to global semantic consistency and implicit logical constraints, without sacrificing efficiency.

- We achieve new state-of-the-art results on multiple reward modeling benchmarks and downstream online reinforcement learning tasks, demonstrating the practical value of JRM as an efficient and scalable reward model for large-scale multimodal alignment.

2. Related Work

Reward Modeling for Generative Alignment. Reward models (RMs) are a core component of reinforcement learning from human or AI feedback (RLHF / RLAIF), where preference signals are mapped to scalar rewards for policy optimization (Christiano et al., 2017; Ouyang et al., 2022). Early approaches mainly adopt discriminative preference learning, typically formulated as pairwise or listwise ranking based on human comparisons (Christiano et al., 2017; Ziegler et al., 2019). These methods are computationally efficient and integrate well with policy optimization algorithms such as PPO, DPO, and GRPO (Schulman et al., 2017; Rafailov et al., 2023; Guo et al., 2025), but their evaluation capability is often limited to surface-level patterns, making them less reliable for tasks requiring global semantic understanding.

In visual generation, reward modeling has been widely adopted for alignment. For text-to-image generation, CLIP-based discriminative models such as PickScore and HPSv2 (Kirstain et al., 2023; Wu et al., 2023) are commonly used to evaluate image-text consistency and aesthetics. Explainable evaluation methods like VIEScore (Ku et al., 2024) leverage multimodal large language models to provide interpretable assessments. While efficient, these models mainly rely on global semantic similarity and struggle with complex structural or logical constraints.

Image editing poses higher requirements on reward models, as evaluation must verify consistency between pre- and post-edit images. Recent advances in unified multimodal models (Xiao et al., 2025; Deng et al., 2025; Seedream et al., 2025; Wu et al., 2025a; Labs et al., 2025) have demonstrated promising capabilities in both image generation and editing within a single framework. EditReward (Wu et al., 2025d) trains a discriminative ranking model using human preferences; UniPic 2.0 (Wei et al., 2025) further leverages large closed-source models as evaluators to improve performance via online reinforcement learning (Liu et al., 2025a; He et al., 2025); EditScore (Luo et al., 2025) distills reasoning behaviors from large models to reduce inference cost. Despite these advances, most methods still rely on holistic scoring without explicit modeling of fine-grained semantic relations, which can lead to evaluation hallucination in complex editing scenarios.

Chain-of-Thought for Reasoning and Evaluation. Chain-of-Thought (CoT) (Wei et al., 2022; Yao et al.) en-

hances reasoning and interpretability in large models by generating intermediate steps. In alignment, this paradigm is increasingly adopted in LLM-as-a-Judge and VLM-as-a-Judge frameworks (Zhang et al., 2025a; Wang et al., 2025b;a; Ping et al., 2025; Ankner et al.; Comanici et al., 2025) to facilitate step-by-step analysis of semantic consistency and logical correctness, excelling in tasks requiring complex cross-modal understanding.

However, the significant computational overhead of explicit CoT generation limits its feasibility for large-scale online reinforcement learning. The trade-off between advanced reasoning capabilities and inference efficiency thus remains a pivotal challenge in reward modeling.

Latent Reasoning and Internalized Chain-of-Thought. Recent studies have explored internalizing reasoning processes into model representations, termed as latent reasoning or internalized Chain-of-Thought. Prior work demonstrates that through joint training or auxiliary supervision, models can acquire implicit reasoning capabilities without explicit text generation (Deng et al., 2023). In language models, strong reasoning supervision during training has been shown to improve downstream performance even when CoT generation is disabled at inference time (Lou et al., 2025; Yang et al., 2025), suggesting that reasoning ability can be encoded in high-dimensional representations.

Nevertheless, latent reasoning remains underexplored in reward modeling, particularly for efficiently injecting reasoning capabilities into discriminative models for cross-image semantic alignment. The proposed Joint Reward Modeling (JRM) framework bridges this gap by internalizing CoT-style reasoning into a shared backbone via joint optimization of language and reward objectives, thereby enhancing semantic evaluation while preserving discriminative inference efficiency.

3. Methodology

3.1. Training Data and Supervision Signals

JRM is trained on multimodal data with both preference supervision and language-based semantic supervision. Each sample consists of an input image (or image pair), an editing instruction, and quality or preference annotations.

Preference annotations are used to learn relative reward rankings. Language annotations provide global semantic and consistency constraints. In practice, we build upon existing image editing reward datasets (Wu et al., 2025d) and augment them with automated multimodal evaluation models (Bai et al., 2023; 2025) to generate explanatory language supervision.

The construction process encourages attention to instruction-

relevant regions and enforces semantic consistency across samples. Importantly, JRM does not rely on any specific evaluator or annotation strategy. These signals serve only as scalable sources of semantic supervision during training.

3.2. Model Architecture and Joint Objective

JRM adopts a shared vision-language backbone with task-specific output heads. Given an image x and instruction c , the backbone encoder produces a shared representation:

$$\mathbf{h} = E(x, c). \quad (1)$$

A lightweight discriminative head maps \mathbf{h} to a scalar reward score:

$$r = f_\theta(\mathbf{h}), \quad (2)$$

which is used for preference ranking. A conditional language head models the generation of semantic evaluations:

$$p(y | x, c) = g_\phi(\mathbf{h}). \quad (3)$$

Reward learning is formulated as a preference ranking problem. To capture potential inconsistencies in annotation, we adopt the uncertainty-aware ranking approach from HPSv3 (Ma et al., 2025). By modeling the reward score as a Gaussian distribution $r \sim \mathcal{N}(\mu, \sigma)$, the preference probability becomes:

$$P(x_i \succ x_j | c) = \iint \text{sigmoid}(r_i - r_j) \mathcal{N}(r_i | \mu_i, \sigma_i) \times \mathcal{N}(r_j | \mu_j, \sigma_j) dr_i dr_j, \quad (4)$$

which leads to the ranking loss:

$$\mathcal{L}_{\text{rank}} = -\mathbb{E}_{(i,j)} [\log P(x_i \succ x_j | c)]. \quad (5)$$

The language supervision head minimizes the standard cross-entropy loss over the target explanation y :

$$\mathcal{L}_{\text{LM}} = -\sum_{t=1}^T \log p(y_t | y_{<t}, x, c). \quad (6)$$

The joint training objective is:

$$\mathcal{L}_{\text{total}} = (1 - \alpha) \mathcal{L}_{\text{rank}} + \alpha \mathcal{L}_{\text{LM}}, \quad (7)$$

where α controls the strength of language supervision ($\alpha = 0.7$ for our JRM). Both objectives jointly constrain the shared representation \mathbf{h} : the ranking loss enforces relative order preservation, while the language loss encourages \mathbf{h} to retain global semantic structure.

3.3. Latent Chain-of-Thought and Inference

Joint training encourages the shared representation \mathbf{h} to encode latent semantic factors that determine editing quality, such as instruction satisfaction and global consistency.

The ranking loss requires these factors to support stable preference ordering, while the language loss enforces that they are sufficient for generating structured semantic evaluations. As a result, reasoning capability is internalized into the representation space and can be accessed by a lightweight discriminative head:

$$r = f_{\theta}(\mathbf{h}_{\text{CoT}}). \quad (8)$$

We refer to this implicit reasoning process as **Latent Chain-of-Thought (Latent CoT)**. Unlike explicit Chain-of-Thought methods, Latent CoT does not require generating intermediate reasoning text at inference time. Language supervision acts as an implicit constraint on the representation space, preventing collapse to shallow features:

$$\text{rank}(\text{Cov}(\mathbf{h})) \uparrow \quad \text{under joint training.} \quad (9)$$

We empirically validate this hypothesis in Section 4.3, where joint training nearly doubles the effective rank compared to the baseline.

During inference, JRM uses only the backbone and reward head:

$$r = f_{\theta}(E(x, c)), \quad (10)$$

which ensures low-latency evaluation. The language head can be enabled for diagnostic purposes but does not affect reward computation. For training details, see Figure 5 and Appendix B.

4. Experiments

This section systematically evaluates the effectiveness of Joint Reward Modeling (JRM) from five perspectives. We first validate JRM’s overall performance advantages on standard reward model benchmarks and reveal its key mechanisms (Latent CoT) through ablation experiments. Subsequently, we analyze the internal representation structure from a representation space perspective to verify whether implicit reasoning capability has been effectively injected into the shared backbone. Furthermore, we demonstrate JRM’s capabilities in self-diagnosis and self-correction scenarios to analyze the quality of semantic representations learned by the shared backbone. Finally, we evaluate JRM’s robustness and efficiency in downstream online reinforcement learning tasks to verify its applicability in practical optimization loops.

Table 1. Performance on EditReward-Bench. JRM significantly outperforms existing methods while maintaining discriminative inference efficiency.

Method	PF	Cons.	Overall
GPT-4.1	0.673	0.602	0.705
GPT-5	0.777	0.669	0.755
Gemini-2.5-Pro	0.703	0.560	0.722
EditScore-8B	0.608	0.594	0.690
EditScore-72B	0.638	0.586	0.703
PaCo-Reward-7B	0.777	0.709	0.751
Gemini-3.0-Flash	0.717	0.662	0.769
EditReward	0.832	-	0.792
JRM (Ours)	0.854	-	0.851

Table 2. Performance on MMRB2 Benchmark. JRM achieves best performance in both single-image and multi-image scenarios.

Method	Single	Multi	Overall
			Pointwise
Qwen3-VL-8B	0.425	0.393	0.419
Qwen3-VL-32B	0.467	0.461	0.466
Gemini-2.5-Pro	0.545	0.483	0.534
EditScore-8B	0.579	0.528	0.570
Gemini-3.0-Pro	0.594	0.573	0.590
GPT-5	0.627	0.584	0.619
Gemini-3.0-Flash	0.627	0.596	0.621
EditReward	0.672	0.590	0.657
JRM (Ours)	0.703	0.646	0.693

4.1. Performance on Reward Modeling Benchmarks

We evaluate JRM’s performance on multiple public reward model benchmarks (Luo et al., 2025; Hu et al., 2025), covering different types of image editing instructions, semantic complexity, and preference annotation formats. Comparison methods include pure discriminative reward models and generative reward models based on explicit reasoning generation.

As shown in Table 1, JRM achieves significantly better performance than pure discriminative reward models on EditReward-Bench. In the Prompt Following dimension, JRM achieves 85.4% accuracy; in the Overall metric, it reaches 85.1%, a 5.9% improvement over the second-best method, demonstrating strong comprehensive evaluation capability. Notably, JRM does not introduce any additional language generation process during inference, maintaining the same inference path and computational overhead as baseline discriminative models.

On the MMRB2 benchmark (Table 2), JRM also demonstrates excellent performance. In Pointwise evaluation, JRM achieves the best results across all three dimensions—Single Image, Multi Image, and Overall—with improvements of 3.1%, 5.6%, and 3.6% respectively compared to previous best method. These results indicate that under the same

inference efficiency conditions, introducing joint training significantly improves ranking and scoring performance for reward models.

4.2. Impact of Language Supervision Weight (α)

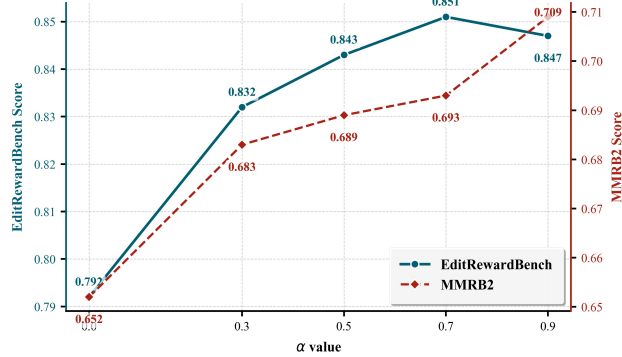


Figure 4. Impact of different language supervision weights α on model performance. As α increases, model performance steadily improves on both benchmarks. Note: except for $\alpha = 0.7$ (the chosen setting for JRM), the optimal checkpoints differ between the two benchmarks; results shown represent the best performance achieved on each benchmark respectively.

To analyze the impact of language supervision signals on reward model performance, we systematically adjust the weight α of the language modeling term in the joint loss function and report corresponding performance changes on the same evaluation benchmarks. All other training configurations remain consistent except for α .

Experimental results shown in Figure 4 demonstrate that as α increases, JRM shows stable improvement trends in accuracy and consistency metrics across multiple benchmarks.

These results indicate that language supervision signals have a significant impact on reward model performance during joint training. Their role is not limited to regularization but is closely related to the quality of intermediate representations learned by the model.

Figure 5 illustrates the training dynamics of both loss components. Notably, when $\alpha > 0$ (with language supervision), the ranking loss converges faster and more stably than the baseline ($\alpha = 0$), suggesting that language supervision provides beneficial inductive bias for reward learning. Meanwhile, the cross-entropy loss converges smoothly, indicating that the two objectives are complementary rather than conflicting.

4.3. Representation Analysis via Singular Value Decomposition

To further analyze JRM’s impact on the internal representations of reward models, we perform comparative analysis between JRM and baseline reward models from a represen-

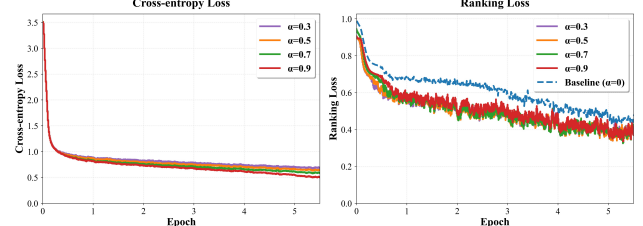


Figure 5. Training dynamics of component losses. **Left:** Cross-entropy loss (language supervision). **Right:** Ranking loss under different α values.

tation space perspective. Specifically, while maintaining consistent model structure and inference flow, we use both the baseline reward model ($\alpha = 0$) and JRM ($\alpha = 0.7$) to evaluate the same batch of image editing results generated by OmniGen2 on GEdit-Bench, extracting hidden representations at corresponding layers of their shared backbone networks. We then perform singular value decomposition (SVD) on the collected feature representations to characterize their information distribution properties in latent space.

Results are shown in Figure 6. Compared to the baseline model, JRM’s singular value spectrum exhibits a more gradual decay trend. The decay rate of singular values reflects whether representations are concentrated in a few principal directions; a flatter spectrum distribution means the model utilizes more principal components for information encoding. Correspondingly, JRM achieves an effective dimension (measuring the number of principal components participating in representation) of 91.77, nearly twice that of the baseline model’s 46.86, indicating that its hidden representations have not collapsed into a low-dimensional subspace.

Furthermore, in statistical metrics such as representation isotropy (characterizing the uniformity of energy distribution across different directions) and spectral entropy (measuring representation distribution complexity from an information-theoretic perspective), JRM consistently outperforms baseline models. This indicates that its latent space structure is more balanced and capable of encoding richer semantic and logical information rather than being dominated by simple heuristic features.

From a semantic perspective, the higher-dimensional and more dispersed topological structure shown in the PCA plots indicates that the model can simultaneously encode rich global semantic and logical factors in its hidden space rather than collapsing onto local surface-level cues. This intuitively validates the design intent of JRM: injecting implicit reasoning supervision through joint language modeling to reshape backbone representations.

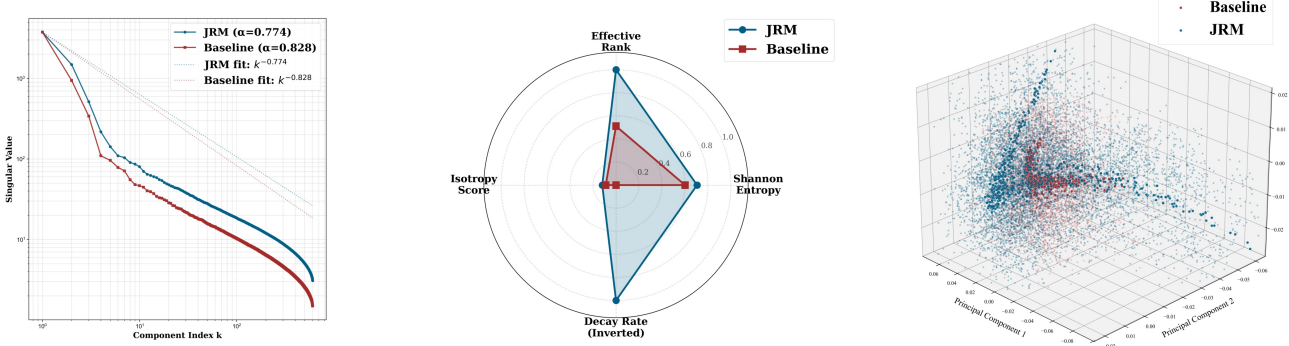


Figure 6. Representation space analysis. **Left:** Singular value spectrum comparison: JRM (blue) exhibits a significantly flatter decay compared to the baseline (red), indicating higher-dimensional information encoding. **Middle:** Representation quality metrics: JRM achieves substantially higher effective rank (91.77 vs. 46.86), spectral entropy, and isotropy score, confirming that joint training prevents representation collapse. **Right:** 3D PCA visualization of hidden states with Procrustes alignment: JRM representations (blue) are more dispersed across the space, while baseline representations (red) tend to collapse into a concentrated cluster.

Table 3. Self-Correction Performance at Different Quality Thresholds. Lower initial VIEScore indicates more challenging samples. JRM-guided correction shows consistent improvements across all difficulty levels.

VIEScore Threshold	Samples	VIEScore Δ	JRM Δ
< 7.0	254	+0.44	+0.28
< 6.0	208	+0.70	+0.26
< 5.0	169	+1.23	+0.28
< 4.0	107	+2.04	+0.39
< 3.0	91	+2.39	+0.43

4.4. JRM-Guided Self-Correction Analysis

This experiment analyzes JRM’s behavioral characteristics on editing results with semantic defects. The specific procedure is as follows: we select challenging samples with low VIEScore from image editing results generated by OmniGen2 (Wu et al., 2025b) on GEdit-Bench (Liu et al., 2025b); then, with the language head enabled, we input the results to JRM to generate natural language evaluations; next, we use this evaluation as an additional condition to guide the editing model for correction; finally, with the language head disabled, we use only the score head to evaluate the images before and after correction.

As shown in Table 3 and Figure 7, evaluations generated by the language head can clearly identify specific problems in editing results and remain consistent with corresponding visual evidence. In subsequent correction stages, the editing model generates more semantically consistent results under the guidance of this feedback. The score head assigns significantly higher reward scores to corrected images.

This experiment demonstrates that the language head and score head share the same representation space during training, and that semantic information guided by language su-



Construct the elephant from bricks.



Use abstract color blocks and lines to express the composition.



Remove the person in the middle of the image.



Please remove the woman outside the car while keeping everything else intact.

Figure 7. Qualitative examples of JRM-guided self-correction. JRM identifies semantic defects in initial editing results through its language head, providing detailed feedback that guides the editing model to produce corrected outputs with improved semantic consistency.

pervision can be reflected in the final reward prediction without generating explicit text.

Table 4. Online RL Performance on GEdit-Bench and ImageEdit-Bench. We report the gains (Δ) on OmniGen2 when aligned with different reward models. **JRM** provides the most significant boost in controllability and consistency.

Configuration	GEdition			ImageEdit		
	SC	PQ	Ovrl.	Δ	Ovrl.	Δ
Baselines (Reported in EditScore)						
Base	6.72	7.20	6.28	-	3.40	-
w/ GPT-4.1	7.24	7.40	6.73	+0.45	3.66	+0.26
w/ EditScore-8B	7.28	6.89	6.89	+0.61	3.62	+0.22
Results in Our Environment						
Base (Reprod.)	6.88	7.38	6.42	-	3.44	-
w/ EditReward	7.43	7.89	7.19	+0.77	3.63	+0.19
w/ Baseline($\alpha = 0$)	7.50	7.91	7.24	+0.82	3.67	+0.23
w/ JRM	7.75	8.14	7.42	+1.00	3.94	+0.50

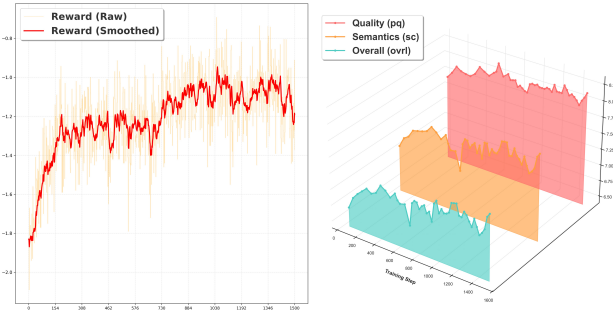


Figure 8. Training dynamics and benchmark evaluation during online RL. **Left:** Reward curves during Flow-GRPO training with JRM, showing steady increase. **Right:** GEdit-Bench scores steadily increase as training progresses, closely tracking the reward dynamics.

4.5. Downstream Online Reinforcement Learning

To validate JRM’s effectiveness as a reward function in practical optimization loops, we fine-tune image editing generation models under online reinforcement learning settings. Specifically, we adopt the Flow-GRPO (Liu et al., 2025a) algorithm and train the same generation model using various open-source and closed-source reward models as well as JRM as reward signals. Experiments are evaluated on two widely-used image editing benchmarks covering multiple practical editing tasks.

As shown in Table 4, on both GEdit-Bench and ImageEdit-Bench (Liu et al., 2025b; Ye et al., 2025) benchmarks, models fine-tuned with JRM for reinforcement learning achieve significantly better performance improvements compared to versions without reinforcement learning. Improvements are particularly notable in semantic consistency-related metrics; stable improvements are also observed in overall perceptual quality metrics.

As illustrated in Figure 8, the reward signal provided by



Figure 9. Qualitative comparison of RL-finetuned models. OmniGen2 aligned with JRM demonstrates superior semantic understanding.

JRM exhibits a steady increase during RL training, and the evaluation scores on GEdit-Bench closely align with the reward curves. This strong correlation validates the accuracy and reliability of JRM as a reward model. For more training details, see Appendix B. Figure 9 further demonstrates that OmniGen2 aligned with JRM acquires enhanced semantic understanding capabilities, correctly interpreting complex instructions involving materials, textures, and spatial relationships. For more qualitative cases, please refer to Appendix D.

5. Conclusion

This paper proposes **Joint Reward Modeling (JRM)**, a new paradigm for enhancing semantic understanding capability while maintaining the efficient inference of discriminative reward models. Through joint training of language generation tasks and reward prediction tasks, the model implicitly learns high-level semantic and logical reasoning capabilities in the shared backbone, without needing to explicitly generate intermediate steps at inference time. Experimental results show that JRM significantly outperforms traditional discriminative models on multiple standard reward model benchmarks and achieves stable and consistent performance improvements in downstream online reinforcement learning tasks. Overall, this method demonstrates that reasoning

capability need not exist in the form of explicit output to be effectively utilized, providing a feasible solution for efficient and scalable reward modeling and alignment, while offering new insights for achieving Efficient Alignment in resource-constrained environments.

References

Ankner, Z., Paul, M., Cui, B., Chang, J. D., and Ammanabrolu, P. Critique-out-loud reward models. In *Pluralistic Alignment Workshop at NeurIPS 2024*.

Bai, J., Bai, S., Yang, S., Wang, S., Tan, S., Wang, P., Lin, J., Zhou, C., and Zhou, J. Qwen-vl: A versatile vision-language model for understanding, localization, text reading, and beyond, 2023. URL <https://arxiv.org/abs/2308.12966>.

Bai, S., Cai, Y., Chen, R., Chen, K., Chen, X., Cheng, Z., Deng, L., Ding, W., Gao, C., Ge, C., Ge, W., Guo, Z., Huang, Q., Huang, J., Huang, F., Hui, B., Jiang, S., Li, Z., Li, M., Li, M., Li, K., Lin, Z., Lin, J., Liu, X., Liu, J., Liu, C., Liu, Y., Liu, D., Liu, S., Lu, D., Luo, R., Lv, C., Men, R., Meng, L., Ren, X., Ren, X., Song, S., Sun, Y., Tang, J., Tu, J., Wan, J., Wang, P., Wang, P., Wang, Q., Wang, Y., Xie, T., Xu, Y., Xu, H., Xu, J., Yang, Z., Yang, M., Yang, J., Yang, A., Yu, B., Zhang, F., Zhang, H., Zhang, X., Zheng, B., Zhong, H., Zhou, J., Zhou, F., Zhou, J., Zhu, Y., and Zhu, K. Qwen3-vl technical report, 2025. URL <https://arxiv.org/abs/2511.21631>.

Christiano, P. F., Leike, J., Brown, T. B., Martic, M., Legg, S., and Amodei, D. Deep reinforcement learning from human preferences. In *Proceedings of the 31st International Conference on Neural Information Processing Systems*, pp. 4302–4310, 2017.

Comanici, G., Bieber, E., Schaeckermann, M., Pasupat, I., Sachdeva, N., Dhillon, I., Blistein, M., Ram, O., Zhang, D., Rosen, E., et al. Gemini 2.5: Pushing the frontier with advanced reasoning, multimodality, long context, and next generation agentic capabilities. *arXiv preprint arXiv:2507.06261*, 2025.

Deng, C., Zhu, D., Li, K., Gou, C., Li, F., Wang, Z., Zhong, S., Yu, W., Nie, X., Song, Z., et al. Emerging properties in unified multimodal pretraining. *arXiv preprint arXiv:2505.14683*, 2025.

Deng, Y., Prasad, K., Fernandez, R., Smolensky, P., Chaudhary, V., and Shieber, S. M. Implicit chain of thought reasoning via knowledge distillation. *CoRR*, 2023.

Gong, Y., Wang, X., Wu, J., Wang, S., Wang, Y., and Wu, X. Onereward: Unified mask-guided image generation via multi-task human preference learning. *arXiv preprint arXiv:2508.21066*, 2025.

Guo, D., Yang, D., Zhang, H., Song, J., Zhang, R., Xu, R., Zhu, Q., Ma, S., Wang, P., Bi, X., et al. Deepseek-r1: Incentivizing reasoning capability in llms via reinforcement learning. *arXiv preprint arXiv:2501.12948*, 2025.

He, X., Fu, S., Zhao, Y., Li, W., Yang, J., Yin, D., Rao, F., and Zhang, B. Tempflow-grpo: When timing matters for grpo in flow models. *arXiv preprint arXiv:2508.04324*, 2025.

Hu, Y., Askari-Hemmat, R., Hall, M., Dinan, E., Zettlemoyer, L., and Ghazvininejad, M. Multimodal reward-bench 2: Evaluating omni reward models for interleaved text and image. *arXiv preprint arXiv:2512.16899*, 2025.

Kirstain, Y., Polyak, A., Singer, U., Matiana, S., Penna, J., and Levy, O. Pick-a-pic: An open dataset of user preferences for text-to-image generation. *Advances in neural information processing systems*, 36:36652–36663, 2023.

Ku, M., Jiang, D., Wei, C., Yue, X., and Chen, W. Viescore: Towards explainable metrics for conditional image synthesis evaluation. In *Proceedings of the 62nd Annual Meeting of the Association for Computational Linguistics (Volume 1: Long Papers)*, pp. 12268–12290, 2024.

Labs, B. F., Batifol, S., Blattmann, A., Boesel, F., Consul, S., Diagne, C., Dockhorn, T., English, J., English, Z., Esser, P., et al. Flux. 1 kontext: Flow matching for in-context image generation and editing in latent space. *arXiv preprint arXiv:2506.15742*, 2025.

Liu, J., Liu, G., Liang, J., Li, Y., Liu, J., Wang, X., Wan, P., Zhang, D., and Ouyang, W. Flow-grpo: Training flow matching models via online rl. *arXiv preprint arXiv:2505.05470*, 2025a.

Liu, S., Han, Y., Xing, P., Yin, F., Wang, R., Cheng, W., Liao, J., Wang, Y., Fu, H., Han, C., et al. Step1x-edit: A practical framework for general image editing. *arXiv preprint arXiv:2504.17761*, 2025b.

Lou, C., Sun, Z., Liang, X., Qu, M., Shen, W., Wang, W., Li, Y., Yang, Q., and Wu, S. Adacot: Pareto-optimal adaptive chain-of-thought triggering via reinforcement learning. *arXiv preprint arXiv:2505.11896*, 2025.

Luo, X., Wang, J., Wu, C., Xiao, S., Jiang, X., Lian, D., Zhang, J., Liu, D., et al. Editscore: Unlocking online rl for image editing via high-fidelity reward modeling. *arXiv preprint arXiv:2509.23909*, 2025.

Ma, Y., Wu, X., Sun, K., and Li, H. Hpsv3: Towards wide-spectrum human preference score. In *Proceedings of the IEEE/CVF International Conference on Computer Vision*, pp. 15086–15095, 2025.

Ouyang, L., Wu, J., Jiang, X., Almeida, D., Wainwright, C. L., Mishkin, P., Zhang, C., Agarwal, S., Slama, K., Ray, A., et al. Training language models to follow instructions with human feedback. In *Proceedings of the 36th International Conference on Neural Information Processing Systems*, pp. 27730–27744, 2022.

Ping, B., Jia, C., Luo, M., Xia, C., Shen, X., Dang, Z., and Qian, H. Paco-rl: Advancing reinforcement learning for consistent image generation with pairwise reward modeling. *arXiv preprint arXiv:2512.04784*, 2025.

Rafailov, R., Sharma, A., Mitchell, E., Manning, C. D., Ermon, S., and Finn, C. Direct preference optimization: Your language model is secretly a reward model. *Advances in neural information processing systems*, 36: 53728–53741, 2023.

Schulman, J., Wolski, F., Dhariwal, P., Radford, A., and Klimov, O. Proximal policy optimization algorithms. *arXiv preprint arXiv:1707.06347*, 2017.

Seedream, T., Chen, Y., Gao, Y., Gong, L., Guo, M., Guo, Q., Guo, Z., Hou, X., Huang, W., Huang, Y., et al. Seedream 4.0: Toward next-generation multimodal image generation. *arXiv preprint arXiv:2509.20427*, 2025.

Wang, Y., Li, Z., Zang, Y., Wang, C., Lu, Q., Jin, C., and Wang, J. Unified multimodal chain-of-thought reward model through reinforcement fine-tuning. *arXiv preprint arXiv:2505.03318*, 2025a.

Wang, Y., Zang, Y., Li, H., Jin, C., and Wang, J. Unified reward model for multimodal understanding and generation. *CoRR*, 2025b.

Wei, H., Xu, B., Liu, H., Wu, C., Liu, J., Peng, Y., Wang, P., Liu, Z., He, J., Xietian, Y., et al. Skywork unipic 2.0: Building kontext model with online rl for unified multimodal model. *arXiv preprint arXiv:2509.04548*, 2025.

Wei, J., Wang, X., Schuurmans, D., Bosma, M., Ichter, B., Xia, F., Chi, E. H., Le, Q. V., and Zhou, D. Chain-of-thought prompting elicits reasoning in large language models. In *Proceedings of the 36th International Conference on Neural Information Processing Systems*, pp. 24824–24837, 2022.

Wu, C., Li, J., Zhou, J., Lin, J., Gao, K., Yan, K., Yin, S.-m., Bai, S., Xu, X., Chen, Y., et al. Qwen-image technical report. *arXiv preprint arXiv:2508.02324*, 2025a.

Wu, C., Zheng, P., Yan, R., Xiao, S., Luo, X., Wang, Y., Li, W., Jiang, X., Liu, Y., Zhou, J., et al. Omnigen2: Exploration to advanced multimodal generation. *arXiv preprint arXiv:2506.18871*, 2025b.

Wu, J., Gao, Y., Ye, Z., Li, M., Li, L., Guo, H., Liu, J., Xue, Z., Hou, X., Liu, W., et al. Rewarddance: Reward scaling in visual generation. *arXiv preprint arXiv:2509.08826*, 2025c.

Wu, K., Jiang, S., Ku, M., Nie, P., Liu, M., and Chen, W. Editreward: A human-aligned reward model for instruction-guided image editing. *arXiv preprint arXiv:2509.26346*, 2025d.

Wu, X., Hao, Y., Sun, K., Chen, Y., Zhu, F., Zhao, R., and Li, H. Human preference score v2: A solid benchmark for evaluating human preferences of text-to-image synthesis. *arXiv preprint arXiv:2306.09341*, 2023.

Xiao, S., Wang, Y., Zhou, J., Yuan, H., Xing, X., Yan, R., Li, C., Wang, S., Huang, T., and Liu, Z. Omnigen: Unified image generation. In *Proceedings of the Computer Vision and Pattern Recognition Conference*, pp. 13294–13304, 2025.

Xue, Z., Wu, J., Gao, Y., Kong, F., Zhu, L., Chen, M., Liu, Z., Liu, W., Guo, Q., Huang, W., et al. Dancegrpo: Unleashing grpo on visual generation. *arXiv preprint arXiv:2505.07818*, 2025.

Yang, B., Wen, B., Ding, B., Liu, C., Chu, C., Song, C., Rao, C., Yi, C., Li, D., Zang, D., Yang, F., Zhou, G., Zhang, G., Shen, H., Peng, H., Ding, H., Wang, H., Fan, H., Ju, H., Huang, J., Cao, J., Chen, J., Hua, J., Chen, K., Jiang, K., Tang, K., Gai, K., Wei, M., Wang, Q., Wang, R., Na, S., Zhang, S., Mao, S., Huang, S., Zhang, T., Gao, T., Chen, W., Yuan, W., Wu, X., Hu, X., Lu, X., Zhang, Y.-F., Yang, Y., Chen, Y., Lu, Z., Wu, Z., Ling, Z., Yang, Z., Li, Z., Xu, D., Gao, H., Li, H., Wang, J., Ren, L., Hu, Q., Wang, Q., Wang, S., Luo, X., Li, Y., Hu, Y., and Zhang, Z. Kwai keye-vl 1.5 technical report, 2025. URL <https://arxiv.org/abs/2509.01563>.

Yao, S., Yu, D., Zhao, J., Shafran, I., Griffiths, T. L., Cao, Y., and Narasimhan, K. R. Tree of thoughts: Deliberate problem solving with large language models. In *Thirty-seventh Conference on Neural Information Processing Systems*.

Ye, Y., He, X., Li, Z., Lin, B., Yuan, S., Yan, Z., Hou, B., and Yuan, L. Imgedit: A unified image editing dataset and benchmark. *arXiv preprint arXiv:2505.20275*, 2025.

Zhang, P., Dong, X., Wang, B., Cao, Y., Xu, C., Ouyang, L., Zhao, Z., Duan, H., Zhang, S., Ding, S., et al. Internlm-xcomposer: A vision-language large model for advanced text-image comprehension and composition. *arXiv preprint arXiv:2309.15112*, 2023.

Zhang, Y., Yu, T., Tian, H., Fu, C., Li, P., Zeng, J., Xie, W., Shi, Y., Zhang, H., Wu, J., et al. Mm-rlhf: The next step forward in multimodal llm alignment. In *Forty-second International Conference on Machine Learning*.

Zhang, Y.-F., Lu, X., Hu, X., Fu, C., Wen, B., Zhang, T., Liu, C., Jiang, K., Chen, K., Tang, K., et al. R1-reward:

Training multimodal reward model through stable reinforcement learning. *arXiv preprint arXiv:2505.02835*, 2025a.

Zhang, Y.-F., Yang, H., Zhang, H., Shi, Y., Chen, Z., Tian, H., Fu, C., Wang, H., Wu, K., Cui, B., et al. Basereward: A strong baseline for multimodal reward model. *arXiv preprint arXiv:2509.16127*, 2025b.

Ziegler, D. M., Stiennon, N., Wu, J., Brown, T. B., Radford, A., Amodei, D., Christiano, P., and Irving, G. Fine-tuning language models from human preferences. *arXiv preprint arXiv:1909.08593*, 2019.

A. Language Supervision Data Construction

This section provides the complete prompt templates used to generate structured language supervision signals for joint training. We employ two complementary prompts to evaluate image editing results from different perspectives.

A.1. Instruction Following Evaluation Prompt

INSTRUCTION FOLLOWING DATA CONSTRUCTION TEMPLATE

You are an expert AI training data annotator and visual linguistics specialist. Your task is to generate a structured evaluation entry for an image editing pair based on a pre-assigned score.

****Inputs:****

- **Instruction:** “{instruction}”
- **Assigned Score:** {score} / 4
- **Images:** [Original Image], [Edited Image]

****Job Description:****

1. **Identify Edit Regions (Grounding):**

- Analyze the instruction and the changes in the images to identify **ALL distinct objects or regions** involved in the edit.
- For each distinct edit target (up to k regions), create a bounding box [ymin, xmin, ymax, xmax] (0-1000 scale) and assign it a unique ID starting from 0.
- Example: If the instruction is “Change the cat to a dog and make the grass blue”, identify Region 0 (dog) and Region 1 (grass).

2. **Draft the Reasoning:**

- Write a detailed justification for the score of {score}.
- **Mandatory Tagging:** You MUST reference specific regions using their tags <|bbox_0|>, <|bbox_1|>, ..., <|bbox_k|> immediately before discussing them.
- Use <|global|> to discuss the overall context, background preservation, and composition.

3. **Align with Score {score}:**

- **Score 4:** All <|bbox_k|> regions are edited perfectly. <|global|> background is perfectly preserved.
- **Score 3:** Main goal achieved, but one specific <|bbox_k|> has a minor flaw (e.g., texture/color off), or <|global|> has slight noise.
- **Score 2:** A major <|bbox_k|> is misinterpreted/failed, or <|global|> background is significantly corrupted/over-edited.
- **Score 1:** Complete failure to follow instruction or image collapse.

****Output Format (JSON Only):**

```
{
  "edit_region": [
    {"id": 0, "label": "concise_label_for_first_target",
     "bbox_2d": [ymin, xmin, ymax, xmax]},
    {"id": 1, "label": "concise_label_for_second_target",
     "bbox_2d": [ymin, xmin, ymax, xmax]}
  ],
  "reasoning": "<|bbox_0|> [Detailed analysis of region 0]
  <|bbox_1|> [Detailed analysis of region 1] ...
  <|global|> [Analysis of unedited regions and
  global consistency]"
}
```

A.2. Visual Quality Evaluation Prompt

VISUAL QUALITY DATA CONSTRUCTION TEMPLATE

You are an expert visual quality inspector. Your task is to generate a detailed critique of an AI-generated image based on a pre-assigned quality score.

****Inputs:****

- **Assigned Score:** {score} / 4
- **Image:** [Edited Image]

****Job Description:**

Analyze the image strictly for **Visual Quality** (Physics, Lighting, Artifacts) to justify the score of {score}.

- Do NOT discuss the text instruction.
- **Score 4 details:** Mention perfect lighting, realistic textures, and no artifacts.
- **Score 3 details:** Mention high quality but verify a specific minor flaw (e.g., “slight noise in shadow”).
- **Score 2 details:** Point out obvious flaws like “distorted face,” “blurred edges,” or “inconsistent shadows.”
- **Score 1 details:** Describe severe failure (garbage output).

****Output Format (JSON Only):**

```
{
  "reasoning": "[Detailed reasoning text describing
    the style, lighting, and any artifacts.
    Be specific about why it receives
    a score of {score}.]"
}
```

B. Training and Implementation Details

B.1. Joint Reward Model Training

Training Hyperparameters. JRM is fine-tuned from the Qwen3-VL-8B-Instruct model. All experiments are conducted using PyTorch 2.5.1 and Transformers 4.56.1.

- **Optimizer:** AdamW ($\beta_1 = 0.9$, $\beta_2 = 0.95$)
- **Weight Decay:** 0.1
- **Peak Learning Rate:** 2×10^{-6}
- **Learning Rate Schedule:** Cosine decay with 5% warmup ratio
- **Training Epochs:** 10
- **Global Batch Size:** 64 (per-device batch size 2, gradient accumulation 4, across 8 GPUs)
- **Maximum Sequence Length:** 8192
- **Image Resolution:** Adaptive (200,704 pixels, equivalent to $256 \times 28 \times 28$)
- **Joint Loss Weight α :** 0.7
- **Precision:** Mixed-precision (bfloating16)
- **Gradient Checkpointing:** Enabled (non-reentrant mode)
- **Distributed Training:** DeepSpeed ZeRO-2

Model Architecture. The reward model adopts a multi-head architecture with a RankNet-style discriminative head for preference ranking and a conditional language generation head for semantic explanation. We employ a learnable special token appended to the input sequence, whose final hidden state serves as the shared representation h . The reward head outputs 2-dimensional scores for instruction following and visual quality.

Compute Resources. Training is conducted on 8 GPUs. The full training process takes approximately 40-50 GPU hours.

Training Dynamics. Figure 10 illustrates the gradient norm stability across different language supervision weights α . While joint training with language supervision introduces larger initial gradient norms (particularly for higher α values), all variants rapidly stabilize within the first epoch. Notably, the baseline ($\alpha = 0$) maintains consistently low gradient norms throughout training, whereas configurations with language supervision exhibit richer gradient signals that facilitate representation learning.

Figure 11 shows the late-stage convergence behavior of total loss. Although higher α values result in larger absolute loss

(due to the additional language modeling objective), all configurations demonstrate stable convergence. The $\alpha = 0.3$ configuration achieves the lowest final loss value, while $\alpha = 0.7$ (our chosen setting) provides an optimal balance between convergence speed and downstream task performance.

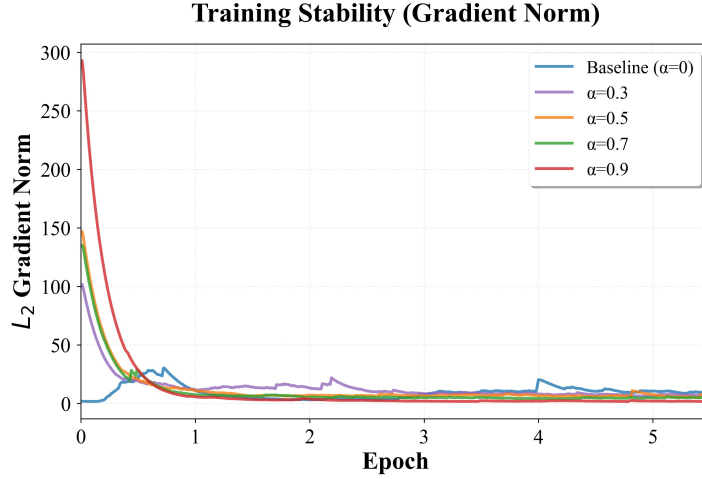


Figure 10. **Gradient norm stability during JRM training.** Higher α values lead to larger initial gradients but converge rapidly within the first epoch.

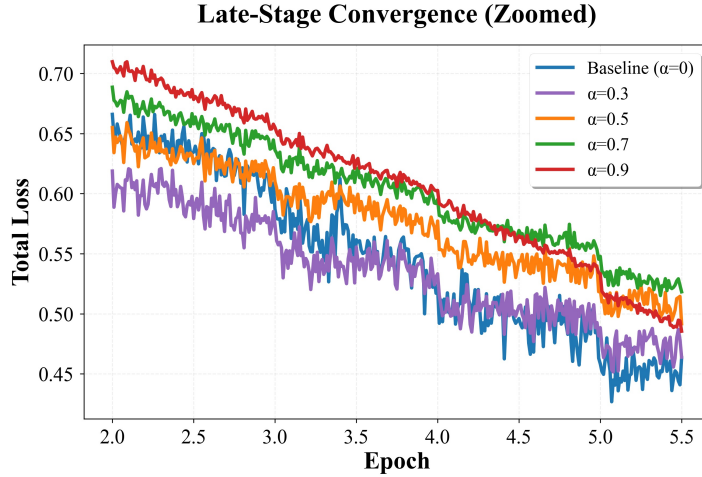


Figure 11. **Late-stage loss convergence (epochs 2–5.5).** All configurations show stable convergence, with lower α achieving lower final loss values.

B.2. Reinforcement Learning Fine-Tuning

Training Hyperparameters. For online RL fine-tuning of OmniGen2-Edit, we use the Flow-GRPO algorithm.

- **Algorithm:** Flow-GRPO (Group Relative Policy Optimization)
- **Discrete Timesteps T :** 20
- **Diffusion Coefficient σ :** 0.9
- **Global Batch Size:** 288
- **Group Size G :** 12
- **PPO Clipping ϵ_{low} :** 10^{-4}
- **PPO Clipping ϵ_{high} :** 5×10^{-4}
- **Learning Rate:** 4×10^{-4}
- **KL Penalty Coefficient β :** 0.04

- **LoRA Configuration:** $r = 32, \alpha = 64$

Compute Resources. Online RL fine-tuning is performed on 32 GPUs with iterative sampling and policy updates. The detailed loss dynamics during training are illustrated in Figure 12.

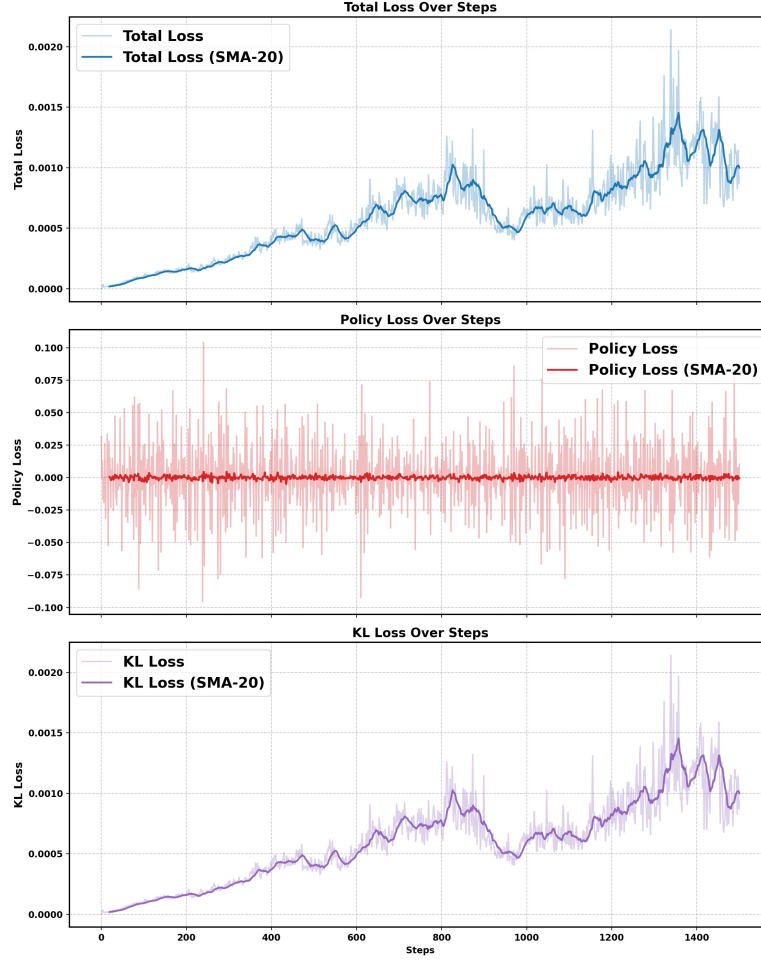


Figure 12. Loss components during Flow-GRPO training. The figure shows the dynamics of individual loss terms during online RL fine-tuning with JRM as the reward signal.

C. JRM Inference Prompts

At inference time, JRM can optionally generate language evaluations through the language head. Below are the complete prompt templates used for each evaluation dimension.

C.1. Instruction Following Inference Prompt

INSTRUCTION EDIT FOLLOWING TEMPLATE

You are tasked with evaluating an edited image **in comparison with the original source image** based on **Instruction Following & Semantic Fidelity**, and assigning a score from 1 to 4, with 1 being the worst and 4 being the best. This dimension focuses on how accurately, completely, and exclusively the model executed the given text instruction.

**Inputs Provided:

- Source Image (before editing)
- Edited Image (after applying the instruction)
- Text Instruction

**Sub-Dimensions to Evaluate:

- **Semantic Accuracy:** Assess whether the edited content accurately captures the semantics of the instruction. The edited result should precisely match the intended meaning. For example, if the instruction is “replace apples with oranges,” the object must clearly be oranges, not other fruits.
- **Completeness of Editing:** Check whether **all parts** of the instruction are fully executed. For multi-step edits (e.g., “replace a red car with a blue bicycle”), both the color change and the object replacement must be done without omissions.
- **Exclusivity of Edit (No Over-Editing):** Ensure that only the requested parts are changed. The rest of the image (as seen in the source) should remain unaltered. For example, if the instruction only involves replacing an object, the background, lighting, and unrelated objects should not be unnecessarily modified.

**Scoring Criteria:

- **4 (Very Good):** Perfectly accurate, complete, and exclusive execution of the instruction.
- **3 (Relatively Good):** Largely correct, but with minor omissions or slight over-editing.
- **2 (Relatively Poor):** Major misinterpretation, incomplete edits, or noticeable unintended changes.
- **1 (Very Poor):** Instruction ignored or completely wrong execution.

**IMPORTANT: Output Format

You must provide your output in this format:

```
{"edit_region": [...], "reasoning": "..."}
```

First, identify where the editing occurred in the second image:

- If editing was successful, provide bounding boxes with labels: `[{"id": 0~n, "label": "description of edited area", "bbox_2d": [x1, y1, x2, y2]}]` (coordinates normalized to [0, 1000] range)
- If editing failed (images look identical), use empty list: `[]`

In your reasoning, use special tokens to reference regions:

- `<|bbox_{id}|>` before describing each edited region (if exist)
- `<|global|>` before overall assessment

Text instruction - {text_prompt}

C.2. Visual Quality Inference Prompt

VISUAL QUALITY EVALUATION TEMPLATE

You are tasked with evaluating an edited image **in comparison with the original source image** based on **Visual Quality & Realism**, and assigning a score from 1 to 4, with 1 being the worst and 4 being the best. This dimension focuses on how realistic, artifact-free, and aesthetically appealing the edited image is, while remaining consistent with the source image.

**Inputs Provided:

- Source Image (before editing)
- Edited Image (after applying the instruction)
- Text Instruction

**Sub-Dimensions to Evaluate:

- **Plausibility & Physical Consistency:** Check whether the edit aligns with the laws of physics and the scene context. Lighting, shadows, reflections, perspective, size, and interactions with the environment should all appear natural compared to the source image.
- **Artifact-Free Quality:** Look for technical flaws such as blur, distortions, pixel misalignment, unnatural textures, or seams around edited regions. High-quality results should be free from such visible artifacts.
- **Aesthetic Quality:** Evaluate the overall harmony and visual appeal. The image should look natural, balanced, and pleasant. Colors, composition, and atmosphere should enhance the image rather than degrade it.

**Scoring Criteria:

- **4 (Very Good):** Perfectly realistic, artifact-free, seamless, and aesthetically pleasing.
- **3 (Relatively Good):** Mostly realistic and clean, with only minor flaws that do not significantly distract.
- **2 (Relatively Poor):** Noticeable physical inconsistencies or visible artifacts that make the edit unnatural.
- **1 (Very Poor):** Severe artifacts, incoherent composition, or visually unusable result.

Text instruction - {text_prompt}

Note that during standard discriminative inference, JRM bypasses the language head and directly outputs reward scores through the efficient discriminative pathway, ensuring low-latency evaluation suitable for online reinforcement learning.

D. Qualitative Comparison of RL-Fine-Tuned Models

This section presents qualitative comparisons of image editing results generated by OmniGen2 models fine-tuned with different reward signals through reinforcement learning. The following figures show side-by-side comparisons across four conditions: the source image, the base OmniGen2 model, the OmniGen2 model fine-tuned with a baseline reward model, and the OmniGen2 model fine-tuned with JRM (Ours).



Figure 13. Qualitative comparison of RL-fine-tuned OmniGen2 models (Part 1/4). From left to right: Source Image, base OmniGen2, OmniGen2 fine-tuned with baseline reward model (w/ Baseline-RL), and OmniGen2 fine-tuned with JRM (w/ JRM).



Figure 14. Qualitative comparison of RL-fine-tuned OmniGen2 models (Part 2/4).



Figure 15. Qualitative comparison of RL-fine-tuned OmniGen2 models (Part 3/4).

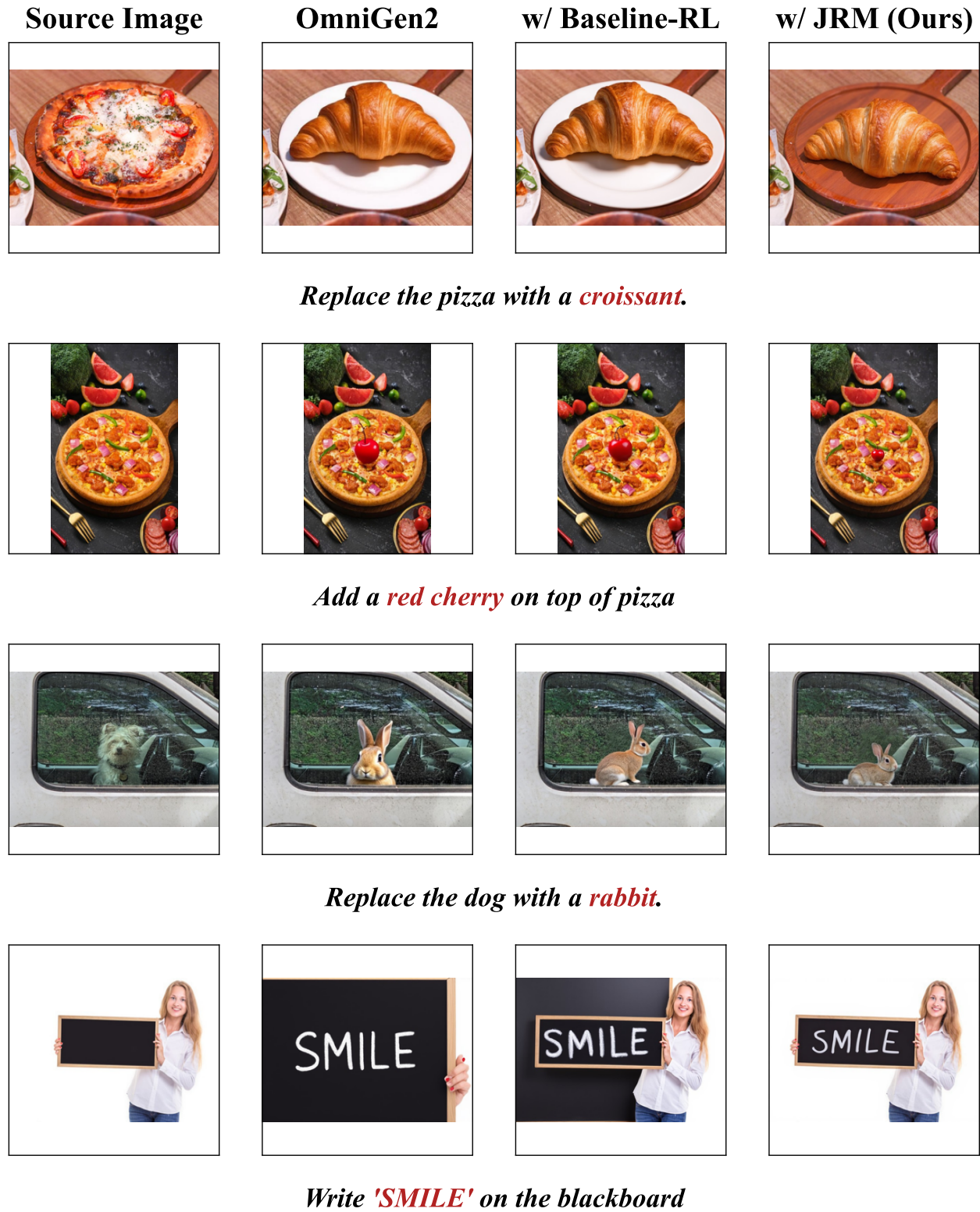


Figure 16. Qualitative comparison of RL-fine-tuned OmniGen2 models (Part 4/4). The JRM-guided model demonstrates superior instruction following and visual quality across diverse editing tasks.